

# Thermotropic Liquid-Crystalline Copolyester/Thermoplastic Elastomer *In Situ* Composites. I. Rheology, Morphology, and Mechanical Properties of Extruded Strands

S. Saikrasun,<sup>1</sup> S. Bualek-Limcharoen,<sup>1</sup> S. Kohjiya,<sup>2</sup> K. Urayama<sup>2</sup>

<sup>1</sup>Department of Chemistry, Faculty of Science, Mahidol University, Rama 6 Road, Bangkok 10400, Thailand

<sup>2</sup>Institute for Chemical Research, Kyoto University, Uji, Kyoto-fu 611-0011, Japan

Received 5 September 2002; accepted 27 November 2002

**ABSTRACT:** A thermotropic liquid-crystalline polymer (TLCP), a copolyester with a 60/40 molar ratio of *p*-hydroxy benzoic acid and poly(ethylene terephthalate), was blended with a styrene/ethylene butylene/styrene thermoplastic elastomer with a twin-screw extruder. The rheological behavior, morphology, and mechanical properties of the extruded strands of the blends were investigated. The rheological measurements were performed on a capillary rheometer in the shear rate range of 5–2000 s<sup>-1</sup> and on a plate-and-plate rheometer in the frequency range of 0.6–200 rad s<sup>-1</sup>. All the neat components and blends exhibited shear thinning behavior. Both the shear and complex viscosities of all the blends decreased with increasing TLCP contents, but the decrease in the shear viscosity was more pronounced. The best fibrillar morphology was observed in the extruded strands of a blend containing 30 wt % TLCP, and a lamellar structure started to form at 40 wt % TLCP. With an increas-

ing concentration of TLCP, the tensile modulus of the blends was greatly enhanced, whereas the tensile strength was almost unchanged. The elongation at break of the blends first slightly decreased with the addition of TLCP and then sharply dropped at 40 wt % TLCP. The tension set measured at 200% deformation slightly increased with increasing TLCP contents up to 30 wt %, over which the set value was unacceptable for a thermoplastic elastomer. A remarkable improvement in the dynamic mechanical properties of the extruded strands was observed in the blends with increasing amounts of TLCP. © 2003 Wiley Periodicals, Inc. *J Appl Polym Sci* 89: 2676–2685, 2003

**Key words:** composites; liquid-crystalline polymers (LCP); thermoplastics; elastomers; rheology; morphology; mechanical properties

## INTRODUCTION

Blending two or more polymers is a versatile way of developing new materials with a desirable combination of properties. Among such blending systems, immiscible blends of thermotropic liquid-crystalline polymers (TLCPs) with thermoplastics are receiving much attention.<sup>1–3</sup> Under an appropriate shear or elongational flow field, dispersed TLCP droplets can be deformed into fibrils, and after quenching for blend solidification, these TLCP fibrils reinforce the matrix as a result of their inherent strength and stiffness. Therefore, this type of blend is called an *in situ* composite.<sup>4</sup> The mechanical properties of the finished

products are closely related to their morphology. There are several important factors affecting the blend morphology, such as the composition, viscosity ratio (dispersed phase to matrix phase), processing conditions, and fabrication techniques. These parameters influence the size, shape, distribution, and molecular orientation of the TLCP phase.

Thermoplastic elastomers (TPEs) are materials that have the processing characteristics of thermoplastics and the elastomeric performance of conventional thermoset rubbers. The increasing number of applications of TPEs are, therefore, due to the ease of processing and fabrication. However, at high temperatures, the strength and dimensional stability of TPEs are not as good as those of conventional vulcanized rubbers. This is due to the fact that the interaction through physical crosslinks in the hard phase becomes weak at elevated temperature. The reinforcement of TPEs by the incorporation of inorganic or organic fibrous fillers has, therefore, gained considerable interest.<sup>5–8</sup> The main aim of this investigation is to improve the strength, modulus of elasticity, and dimensional stability of TPEs at elevated temperatures. Despite the advantages of the incorporation of these short fibers,

Correspondence to: S. Bualek-Limcharoen (scsbl@mahidol.ac.th).

Contract grant sponsor: Royal Golden Jubilee Ph.D. Program; contract grant number: PHD/0111/2542, Thailand Research Fund.

Contract grant sponsor: Postgraduate Education and Research Program in Chemistry.

there are some technical difficulties. The presence of solid fibers in the molten polymer matrix increases the viscosity of the system and causes abrasion on the surface of the processing equipment. Furthermore, some fibers are broken down into fragments because of the high shear stress, and this leads to a significant reduction of the properties of the composite materials. Therefore, blending TPEs with TLCP is interesting because TLCP reduces the melt viscosity of the system and causes no abrasion of the processing equipment because both components are in the melt. The main problem to be investigated is an appropriate processing condition for obtaining a fibrillar morphology in the TLCP phase. So far, only a few TLCP/elastomer blends systems have been investigated.<sup>9–12</sup> Lorenzo et al.<sup>9</sup> reported the viscoelastic behavior of a liquid-crystalline copolyester [60/40 molar ratio of *p*-hydroxy benzoic acid (HBA) to poly(ethylene terephthalate) (PET)] blended with styrene-butadiene rubber. The complex viscosity ( $\eta^*$ ) exhibited minima at 10% TLCP. Verhoogt and coworkers<sup>10,11</sup> studied a blend of Vectra A900 (73% 4-hydroxy benzoic acid/27% 2-hydroxy-6-naphthoic acid) and TPE [styrene/ethylene butylene/styrene (SEBS); Kraton G-1650]. They observed a fibrillar morphology in blends with less than 30 vol % TLCP and found that the addition of TLCP resulted in a substantial increase in both the modulus of elasticity and tensile strength. Moreover, Machiels et al.<sup>12</sup> investigated the fiber formation, stability, and properties of a blend of Vectra A900 with Arnitel em630 [25% poly(oxytetramethylene)/75% poly(butylene terephthalate), a TPE]. In the latter blend system, the tensile modulus and strength increased with an increasing draw ratio of the extrudate as a result of the increase in the fiber aspect ratio and molecular orientation in the TLCP phase.

In this work, we studied a blend of TLCP (60/40 molar ratio of HBA to PET) with SEBS (Kraton G-1652). The aim of this work was to search for appropriate processing conditions and TLCP contents for the preparation of *in situ* reinforced TPEs while important elastomer properties were maintained (i.e., high elongation at break and low tension set value). The morphology and mechanical properties of the blend fabricated as extruded strands and monofilaments were investigated. This article (part I) reports the effect of the TLCP content on the rheological behavior of this blend system and the properties of extruded strands. The results will be compared with those of the monofilaments, which will be reported in part II.

## EXPERIMENTAL

### Materials

The polymer dispersed phase used in this work was Rodrun LC-3000, a TLCP supplied by Unitika Co., Ltd.

(Tokyo, Japan), and the matrix phase was Kraton G-1652, a TPE, kindly provided by Shell Chemical Co. (Houston, TX). Rodrun LC-3000 is a copolyester consisting of HBA and PET (HBA/PET = 60/40 mol/mol). It has a melting point of 220°C and a density of 1.41 g/cm<sup>3</sup>. Kraton G-1652 is an SEBS triblock copolymer with a styrene (S)/rubber ratio of 29/71. The materials were dried in a vacuum oven at 70°C for at least 12 h before use.

### Blending and preparation of the extrudates

The blends of SEBS and TLCP at various compositions were prepared with a corotating, intermeshing, twin-screw extruder (TSE 16-TC, Prism, Staffordshire, United Kingdom) with a screw diameter of 16 mm, a length-to-diameter ratio ( $L/D$ ) of 25, a die diameter of 2 mm, and a screw speed of 60 rpm. The temperature profile was 190–220–220–225–225°C, representing the temperatures at the hopper zone, three barrel zones, and the heating zone in the die head, respectively. The extruded strand was immediately quenched in a water bath and dried in a vacuum oven.

### Measurements of the viscosity

The shear viscosity ( $\eta$ ) measurements of the neat components and blends in the high shear rate range were carried out with a capillary rheometer (RH-7, Rosand, Gloucestershire, England). The measurements were performed in the shear rate range of 5–2000 s<sup>-1</sup> at 225°C, which was equal to the die temperature of the extruder. A long die with a diameter and length of 2 and 24 mm, respectively, and an orifice die were applied for the pressure drop correction.<sup>13</sup> The entry angles of both dies were 90°. The Rabinowitch correction was also applied to calculate the true shear rate.<sup>14</sup>

For  $\eta^*$  measurements with a plate-and-plate rheometer (Rotovisco RT 20, Haake, Karlsruhe, Germany), the extruded strands were cut into small pieces and compression-molded at 200°C into a sheet about 1 mm thick. The sheet was then punched into a disk 20 mm in diameter. The  $\eta^*$  values and complex moduli of all specimens were measured in the oscillatory shear mode within the frequency range of 0.6–200 rad s<sup>-1</sup>. The measuring temperature and the gap between the two plates were set at 225°C and 0.9 mm, respectively.

### Morphology characterization

The fracture surfaces of TLCP/SEBS extruded strands were observed with scanning electron microscopy (SEM; Hitachi 2500, Ibaraki, Japan) operated at an accelerating voltage of 15 kV. Before examination, the extruded strands were dipped in liquid nitrogen for 30 min and fractured. The specimens were sputter-coated with palladium for enhanced surface conductivity.

**TABLE 1**  
**Tensile Properties of the Strands of Neat SEBS and TLCP/SEBS Blends: Modulus at 100% Strain (M100), Modulus at 300% Strain (M300), Tensile Strength (TS), Elongation at Break (EB), and Hardness**

| TLCP/SEBS<br>(w/w) | M100<br>(MPa) | M300<br>(MPa) | TS<br>(MPa) | EB<br>(%) | Hardness<br>(shore A) |
|--------------------|---------------|---------------|-------------|-----------|-----------------------|
| 0/100              | 3.2 ± 0.1     | 5.4 ± 0.2     | 24.6 ± 1.9  | 868 ± 86  | 73.9 ± 0.8            |
| 10/90              | 4.5 ± 0.2     | 8.4 ± 0.2     | 24.8 ± 1.4  | 768 ± 46  | 76.7 ± 0.8            |
| 20/80              | 7.0 ± 0.2     | 11.5 ± 0.4    | 22.9 ± 1.2  | 774 ± 85  | 78.7 ± 0.4            |
| 30/70              | 10.1 ± 0.5    | 13.4 ± 0.5    | 20.9 ± 1.6  | 629 ± 14  | 81.1 ± 0.7            |
| 40/60              | —             | —             | 20.4 ± 2.6  | 5.6 ± 1.9 | 87.5 ± 0.2            |
| 50/50              | —             | —             | 19.7 ± 1.9  | 4.2 ± 1.3 | 87.6 ± 0.3            |

### Tensile testing

The tensile measurements of the extruded strands were performed according to ASTM D 412 on an Instron mechanical tester (model 5569, Instron Corp., Canton, MA) set at a grip length of 25 mm, a crosshead speed of 50 mm/min, and a full-scale load cell of 1000 N. The average value of at least five measurements was determined. The tensile properties measured were the moduli at 100 and 300% strains, the tensile strength, and the elongation at break.

The tension set values of the specimens were determined according to ASTM D 412 with an Instron tensile tester (model 5569) with a grip length of 50 mm. The deformation was applied at 100, 200, and 300% elongation. The mean value of the tension set was determined from five measurements.

In addition, the hardness of all strands was measured according to ASTM D 2240 with a hardness tester (model D7900, Zwick, Ulm, Germany). A load of 12.5 N was applied (Shore A). The specimens were in a cylindrical form about 2 mm in diameter. The mean value of the hardness was determined from six measurements.

### Dynamic mechanical thermal analysis (DMTA)

DMTA was performed on a DVE-V4 Rheospectoler (Rheology, Kyoto, Japan) to obtain the dynamic mechanical storage modulus ( $E'$ ) and the loss tangent ( $\tan \delta = E''/E'$ , where  $E''$  is the dynamic mechanical loss modulus) of the extruded strands. The tensile mode was applied at an oscillating frequency of 10 Hz. The oscillating strain was set at 1% for the blends containing 0–30 wt % TLCP and at 0.2% for the blends containing 40–50 wt % TLCP because the blend became more rigid at higher TLCP levels (see the values of hardness given in Table I). The gauge length was set at 5 mm, and the heating rate was 5°C/min. The measurements were carried out from –100 to 150°C in a flow of nitrogen.  $E'$  and  $\tan \delta$  were recorded as functions of temperature with a detection step of 1°C.

## RESULTS AND DISCUSSION

### Rheological behavior of the blends in the molten state

The  $\eta$  values at 225°C of the neat polymers and the blends containing up to 30 wt % TLCP as a function of the shear rate obtained from a capillary rheometer are presented in Figure 1. The  $\eta^*$  values of the neat polymers and the blends containing up to 50 wt % TLCP as a function of the angular frequency ( $\omega$ ) obtained from a plate-and-plate rheometer are presented in Figure 2. All the flow curves exhibited shear thinning behavior; that is, the viscosity decreased with an increasing shear rate. This was due to the shear-induced chain orientation, leading to a reduction in the chain entanglement and, therefore, a drop in the viscosity. Even with the low shear rate limit examined here, Newtonian behavior was not observed, and this precluded the determination of the zero-shear viscosity for each sample.

For flexible polymers, the curve of  $\eta^*$  as a function of  $\omega$  is identical to the curve of  $\eta$  as a function of the shear rate. This is known as the Cox–Merz rule:<sup>15</sup>

$$|\eta^*(\omega)| = \eta(\dot{\gamma}) \quad (\omega = \dot{\gamma}) \quad (1)$$

This rule fails for some rigid polymers and some polyethylene systems.<sup>16,17</sup> The rheology of a TLCP/PE blend system recently reported by our group obeyed the Cox–Merz rule.<sup>18</sup> In this work, a comparison of the results shown in Figures 1 and 2 reveals that the viscosities of all the pure components and blends showed a significant deviation from the Cox–Merz rule. Both  $\eta$  and  $\eta^*$  of the blends clearly decreased with increasing TLCP contents at all shear rates measured. However, the reduction of the melt viscosity with the addition of TLCP measured by a capillary rheometer was more pronounced than that obtained from a plate-and-plate rheometer. This might be due to the fact that the elongational flow in the capillary further enhanced the molecular orientation in the TLCP phase, and this resulted in a marked reduction in the viscosity.

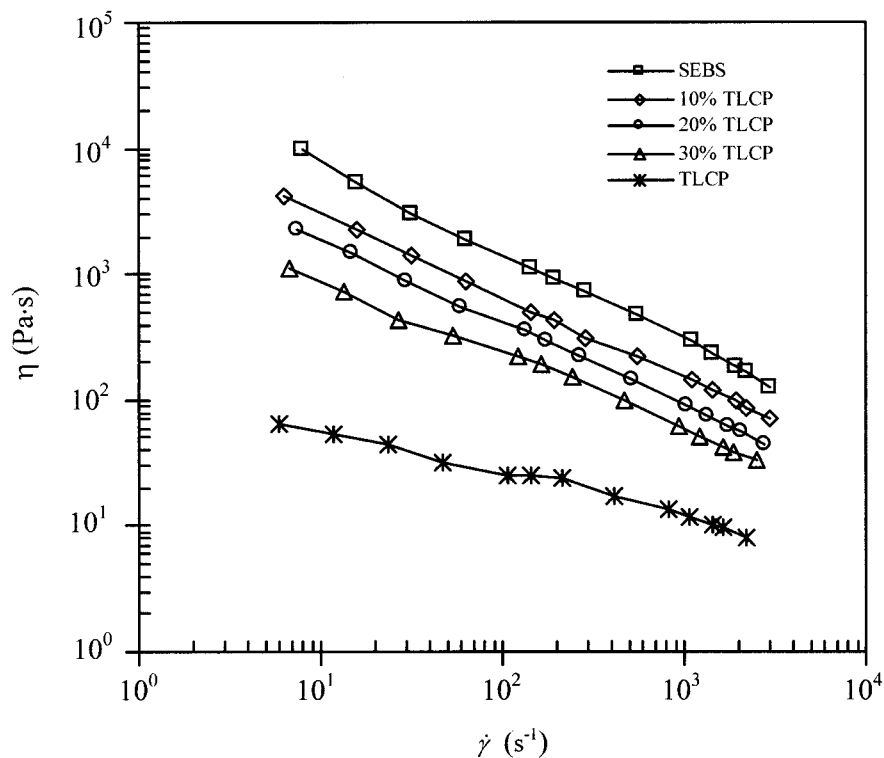


**Figure 1**  $\eta$  versus  $\dot{\gamma}$  for the neat polymers and TLCP/SEBS blends containing various TLCP contents (measured at 225°C with a capillary rheometer).

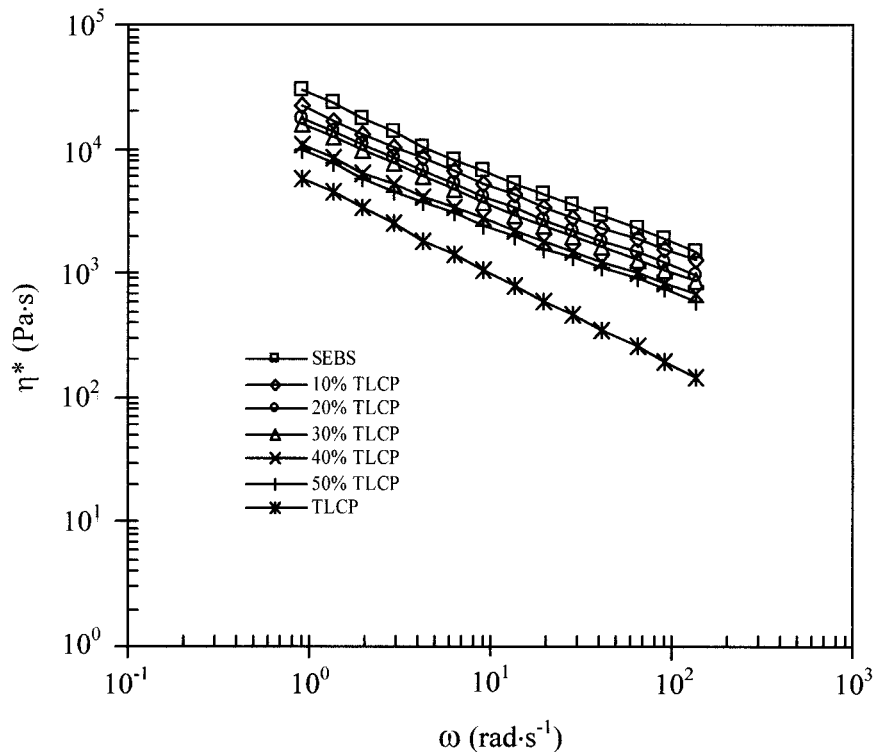


**Figure 2**  $\eta^*$  versus  $\omega$  for the neat polymers and TLCP/SEBS blends containing various TLCP contents (measured at 225°C with a plate-and-plate rheometer).

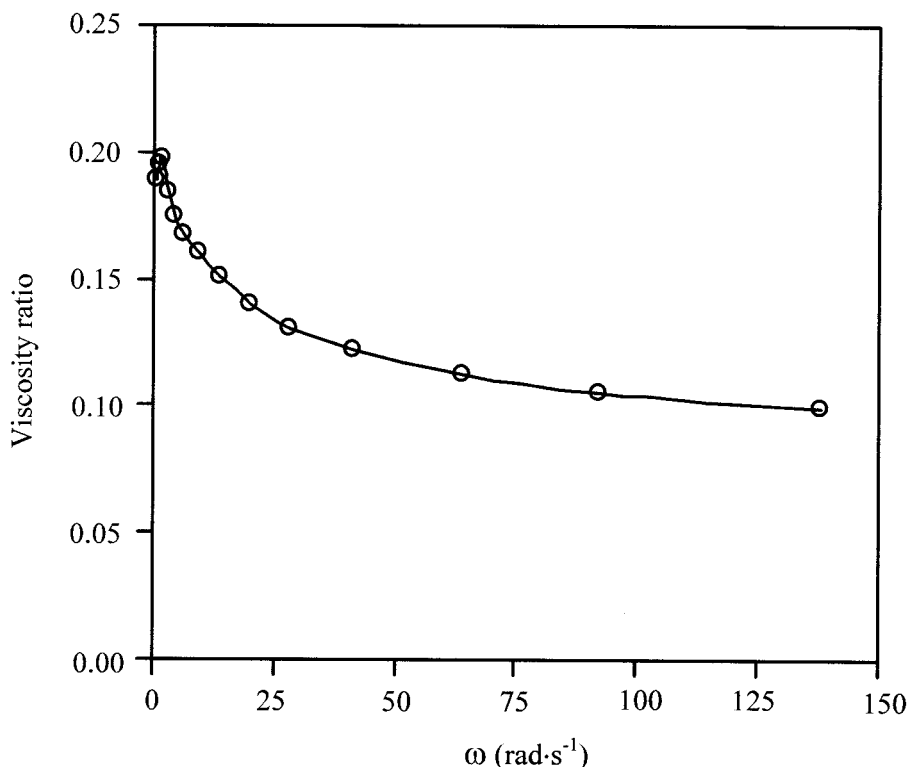


**Figure 3** Viscosity ratio at 225°C versus  $\omega$  (evaluated from data obtained with a plate-and-plate rheometer).

The non-Newtonian behavior in the steady-state flow is normally characterized by the following power law:

$$\eta = k\dot{\gamma}^{(n-1)} \quad (2)$$

where  $n$  is the power-law index. For Newtonian flow ( $n = 1$ ),  $k$  coincides with the zero-shear viscosity.  $n$  was 0.29 for neat SEBS, 0.34 for blends containing 10 and 20 wt % TLCP, 0.41 for 30 wt % TLCP/SEBS blends, and 0.66 for neat TLCP. The degrees of the shear thinning for the blends were comparable to that for neat SEBS, being almost independent of the TLCP content.

Generally, a requirement for the deformation of the dispersed droplets of a polymer melt is that the viscosity ratio of the dispersed polymer to the matrix polymer should be smaller than unity.<sup>19</sup> In this work, the shear rate at the die of the extruder was estimated to be approximately  $100 \text{ s}^{-1}$  at the die temperature of 225°C, and so the viscosity ratio was evaluated from the results obtained from a plate-and-plate rheometer at 225°C. This is presented in Figure 3. The viscosity ratio clearly dropped sharply first and then gradually decreased from 0.19 to 0.10 as  $\omega$  increased from 1 to  $138 \text{ rad s}^{-1}$ . A similar profile of the viscosity ratio was obtained for the rheological behavior of TLCP/PE and TLCP/PP blend systems previously reported by our group.<sup>18,20</sup>

### Morphology

Figure 4 presents SEM micrographs ( $2000\times$  magnification) of fracture surfaces of TLCP/SEBS extruded strands containing various TLCP contents. In the blend with 10 wt % TLCP [Fig. 4(a)], most of the dispersed TLCP domains appeared as droplets, and only a few elongated TLCP domains were seen. The number of elongated TLCP domains increased with increasing TLCP contents, as seen in Figure 4(b,c) for 20 and 30 wt % TLCP, respectively. At 40 and 50 wt % TLCP, a lamellar structure appeared because of the coalescence of liquid TLCP threads that occurred during extrusion. Similarly, Verhoogt et al.<sup>10</sup> reported observing a lamellar structure in a Vectra A900/SEBS blend system with a TLCP content greater than 20 vol %. Of the five specimens shown in Figure 4, the longest TLCP fibers could clearly be seen in the blend containing 30 wt % TLCP with diameters of approximately  $2\text{--}4 \mu\text{m}$ . The fiber-pullout feature revealed poor interaction at the interface because this blend system was immiscible. This is an important requirement for the production of *in situ* composites.

### Tensile properties

The stress-strain curves of neat SEBS and blends with up to 50 wt % TLCP are shown in Figure 5. An increase in the TLCP level led to an enhancement in

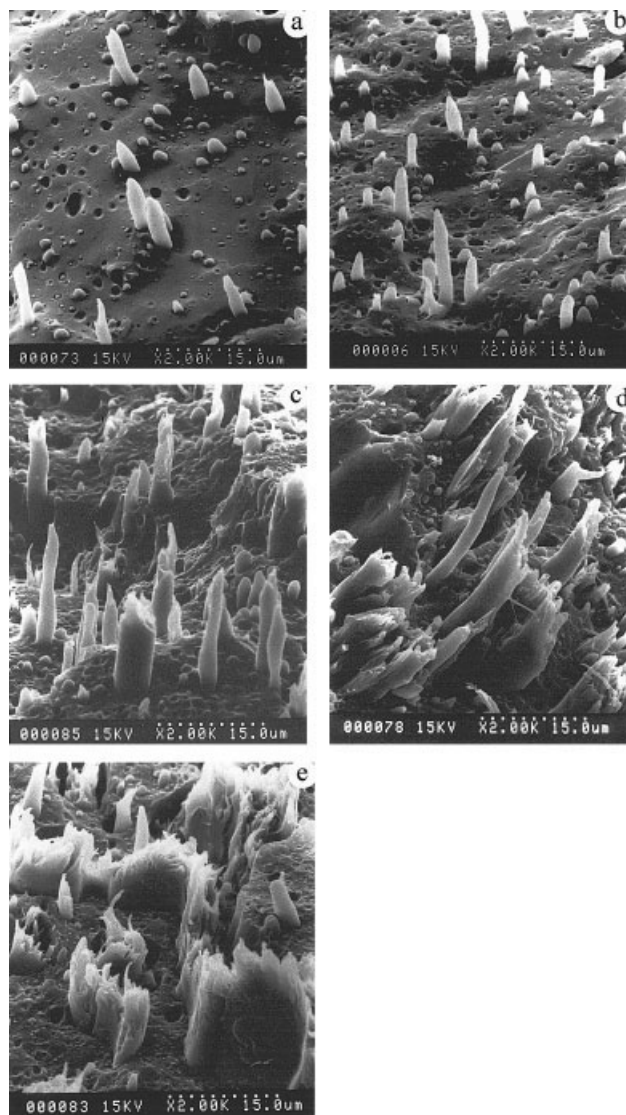


**Figure 4** SEM micrographs of fracture surfaces of extruded strands of TLCP/SEBS blends with (a) 10, (b) 20, (c) 30, (d) 40, and (e) 50 wt % TLCP.

the strength of the blends. The neat SEBS exhibited the lowest stress at all degrees of strain and showed a strain hardening effect. The blends containing up to 30 wt % TLCP still exhibited a good elastic property similar to that of the matrix; that is, the elongation at break was higher than 600%. However, the elongation at break of the blends with 40 wt % TLCP or more dramatically dropped from about 600% to 5%. The sudden drop in the elastic characteristic of the samples with high levels of TLCP might be due to the loss of connectivity in the elastomer phase, and so the blends behaved like plastic materials. This was evident from the lamellar structure in the blends with 40 wt % TLCP or more because the possibility of TLCP liquid threads coalescing during processing increased as the TLCP concentration increased.

The average values of the moduli at 100 and 300% strains, the tensile strength, the elongation at break,

and the hardness are listed in Table I. For the blends containing 10, 20, and 30 wt % TLCP, the moduli linearly increased with increasing TLCP contents. At 100% strain, the improvement in the moduli of the blends containing 10, 20, and 30 wt % TLCP were about 40, 120, and 216%, respectively, when compared with that of the matrix. At 300% strain, the percentage increases in the moduli were 56, 113, and 148%, respectively. This indicates that the SEBS matrix phase was effectively reinforced by TLCP fibrils. The values of the ultimate tensile strength of all the blends were comparable to that of the matrix.

The hardness of the composite strands linearly increased with increasing TLCP contents up to 30 wt % with an increasing step of 2–3 units per 10 wt % TLCP added. Then, a jump of the hardness value occurred at 40 wt % TLCP (an increase of 6 units). This sudden increase agreed with the sudden drop in the value of the elongation at break shown in Figure 5, a characteristic stress–strain behavior for hard and brittle materials.

The tension set is defined as the permanent elongation relative to the original length after a material is stretched to a specified strain for a specified period of time. The effects of the level of applied deformation and the TLCP content on the values of the tension set of the blends containing up to 30 wt % TLCP are shown in Figure 6. Under 100 and 200% strains, the tension set of the specimens slightly increased with increasing levels of TLCP. However, under 300% strain, the tension set increased progressively with the addition of TLCP. In particular, at 30 wt % TLCP, the tension set was about 57%, much higher than the acceptable limit.

In conclusion, the tension sets of all the specimens shown in Figure 6 were within the acceptable limit of the set values for TPES,<sup>21</sup> except that for the blend containing 30 wt % TLCP under an applied strain of 300%.

### Dynamic mechanical properties

To investigate the strength and stability of polymer materials at high temperatures, we performed DMTA measurements from  $-100$  to  $150^{\circ}\text{C}$ . Figures 7 and 8 present plots of  $E'$  and  $\tan \delta$  versus temperature, respectively, for neat SEBS and blends containing up to 50 wt % TLCP. An examination of Figure 7 shows that the magnitude of  $E'$  decreased with increasing temperature and that all specimens exhibited three state regions: glassy, rubbery, and melting states. The first transition point was due to the glass transition of the ethylene butylene (EB) block in SEBS, which was around  $-45^{\circ}\text{C}$ , and the second transition at about  $100^{\circ}\text{C}$  corresponded to the glass-transition temperature ( $T_g$ ) of the S block. In the rubbery (from  $-45$  to  $100^{\circ}\text{C}$ ) and melting ( $>100^{\circ}\text{C}$ ) states,  $E'$  increased with

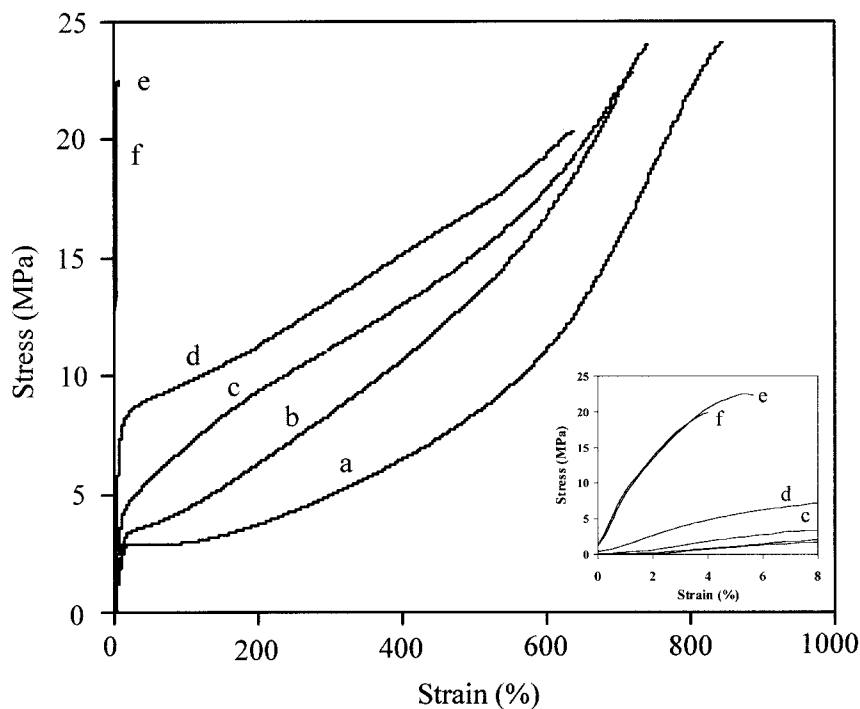


**Figure 5** Stress-strain curves of extruded strands of TLCP/SEBS with (a) 0, (b) 10, (c) 20, (d) 30, (e) 40, and (f) 50 wt % TLCP.

the addition of TLCP because of the reinforcement of TLCP fibrils.

The blend with 30 wt % TLCP showed a big jump in the value of  $E'$  in all states. In the rubbery state, in

particular, it increased by a factor of 7. This result agreed well with the jump in the tensile modulus at a low strain [Fig. 5(d)]. This was again supported by the morphology of the fracture surface [Fig. 4(c)], which

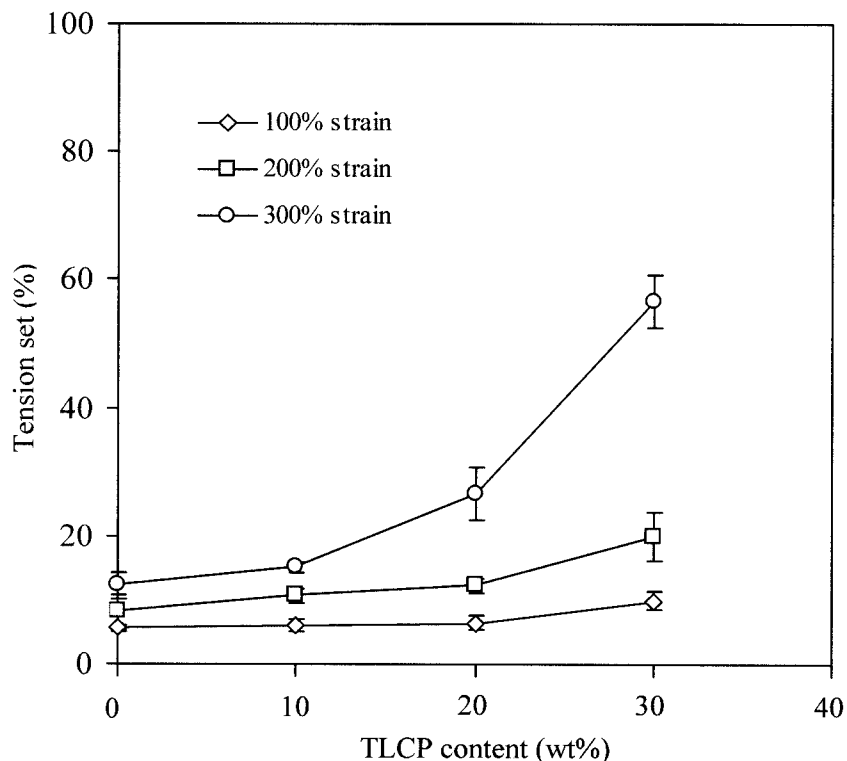


**Figure 6** Tension set values of extruded strands of TLCP/SEBS versus the TLCP content (the measurements were performed at strains of 100, 200, and 300%).

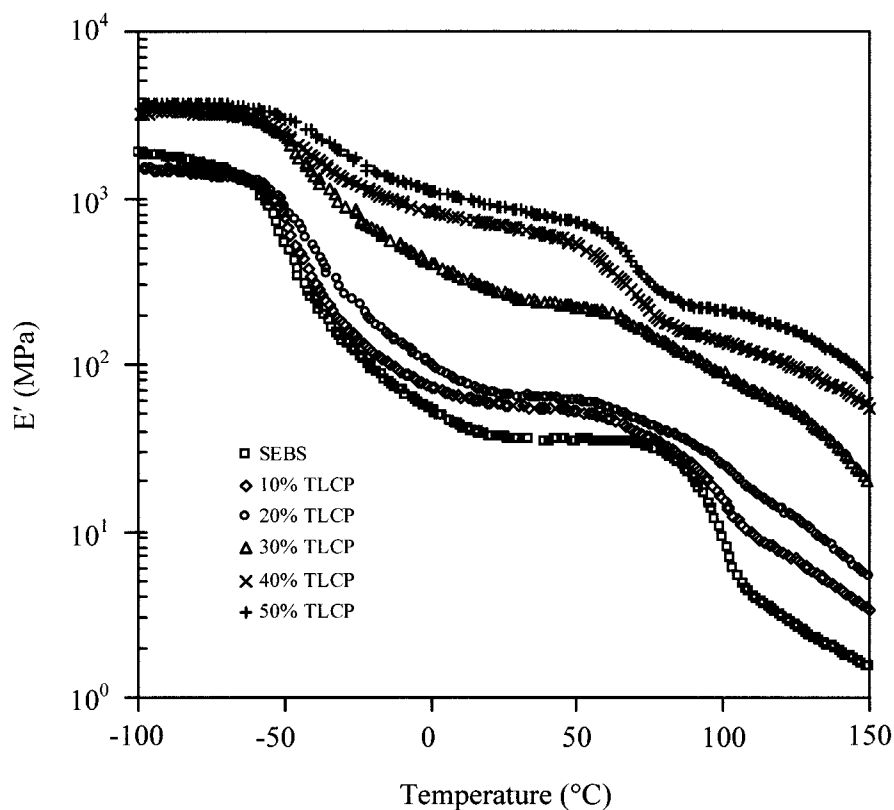


Figure 7  $E'$  as a function of temperature for extruded strands containing various TLCP contents.

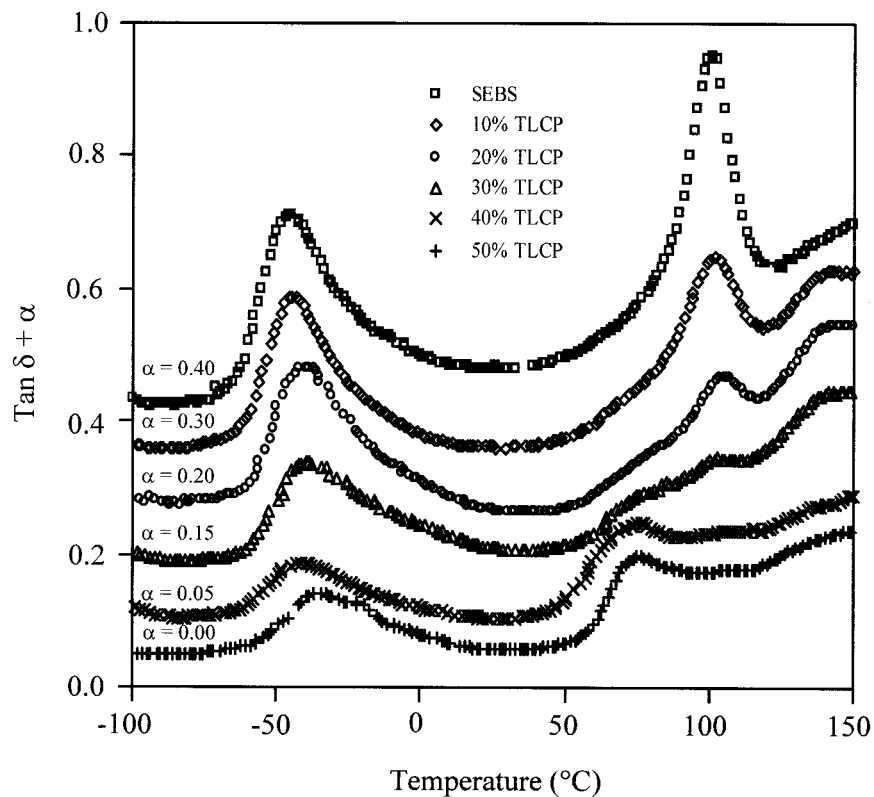


Figure 8  $\text{Tan } \delta$  as a function of temperature for extruded strands containing various TLCP contents ( $\alpha$  is the shift factor).



showed the longest TLCP fibers in comparison with the other blend compositions. The increase in the  $E'$  values with the addition of TLCP indicated an improvement in both the strength and thermal stability at high temperatures. Verhoogt et al.<sup>10</sup> investigated the dynamic mechanical properties of a Vectra A900/SEBS G-1650 blend. They found that the increase of  $E'$  in the blend containing 25 vol % Vectra at room temperature (25°C) was about 200% compared with that of the neat matrix. In this study, for the 30 wt % TLCP/SEBS G-1652 blend (22 vol % TLCP),  $E'$  was about 650% higher than that of the matrix. The better improvement of  $E'$  in our blend system might be due to the higher degree of TLCP fibrillation, whereas some lamellar structure was found in the Vectra A900/SEBS G-1650 blend.<sup>10</sup>

The Halpin-Tsai equation<sup>22</sup> is often used to predict the theoretical modulus of fiber-reinforced composites. The assumption is made that a continuity of stress and strain exists along the interface during testing:

$$\frac{E_c}{E_m} = \frac{1 + ABX}{1 - BX} \quad (3)$$

where

$$B = \frac{E_f/E_m - 1}{E_f/E_m + A} \quad (4)$$

and  $E_c$ ,  $E_m$ , and  $E_f$  represent the longitudinal moduli of the composite, the matrix, and the dispersed fiber, respectively, and  $X$  is the fiber volume fraction. The quantity  $A$  is equal to  $2(L/D)$ , where  $L/D$  is the length/diameter ratio (aspect ratio) of the fibers. Nakamae et al.<sup>23</sup> calculated the elastic modulus in the crystalline region parallel to the chain axis of Rodrun LC-3000 with an X-ray technique to be 59 GPa. In addition, Itoyama<sup>24</sup> determined the elastic modulus of as-spun Rodrun LC-3000 prepared with an applied extension ratio of 1000 with a thermomechanical analyzer to be 50 GPa. To calculate, for instance,  $E_c$  with eqs. (3) and (4) for a 30 wt % TLCP specimen ( $X = 0.22$ ), the values of  $E_f = 59$  GPa,  $E_m = 36$  MPa, and  $L/D = 25$  (assumed) were used. The calculated  $E_c$  value was 534 MPa, much higher than the measured value of 270 MPa (obtained from DMTA data at 25°C, it was approximately the same as Young's modulus). This difference might be due to the broad distribution of  $L/D$  values in the real system. As seen in Figure 4(c), some of the TLCP domains appeared in the form of droplets.

Tan  $\delta$  curves as a function of temperature of the blend extruded strands are shown in Figure 8. Each tan  $\delta$  curve was shifted in the vertical axis by different shift factors ( $\alpha$ ) to prevent overlapping. SEBS showed two peaks around  $-45$  and  $100^\circ\text{C}$  corresponding to

$T_g$ 's of the EB block and S block, respectively. A broad peak with a shoulder at  $-45^\circ\text{C}$  indicated a broad distribution of relaxation times due to the presence of the amorphous EB segments.<sup>25</sup> The  $T_g$  of the EB block in SEBS increased about  $13^\circ\text{C}$  with increasing TLCP contents up to 50 wt %. The  $T_g$  of the S block increased only about  $2^\circ\text{C}$  with increasing TLCP contents up to 30 wt %. For the blends with 40 wt % TLCP or more, the  $T_g$  of the S block could not be detected because of the dilution effect, whereas a new peak appeared at  $73^\circ\text{C}$  corresponding to the  $T_g$  of the PET block in the TLCP component. The shift of the  $T_g$  to a higher temperature might be attributed to a constraint of the SEBS component part that adhered onto TLCP fibers because the aromatic S block in SEBS was expected to be more compatible with TLCP. This was in good agreement with the results reported by Verhoogt et al.<sup>10</sup>

In the next article (part II), we will report the physical properties of the same blend system fabricated as monofilaments subjected to a much higher level of extension. We expect to obtain TLCP fibrils with high aspect ratios and higher levels of improvement in the mechanical properties.

## CONCLUSIONS

The rheological behavior, morphology, and mechanical properties of TLCP/SEBS blends were investigated. The following conclusions could be drawn from this study:

1. The melt viscosity of the blend of TLCP (HBA/PET = 60/40) and SEBS gradually decreased with increasing TLCP contents. All flow curves showed shear thinning behavior.
2. The best fibrillar morphology was achieved when up to 30 wt % TLCP was added. At a higher TLCP concentration, a lamellar structure was formed because of the coalescence of the dispersed phase.
3. The addition of a high-strength TLCP into a TPE SEBS could improve the tensile modulus considerably. The elongation at break fell off somewhat with increasing TLCP contents up to 30 wt % and then dropped sharply at 40 wt % and higher.
4. The characteristic elastic property of the blends containing up to 30 wt % TLCP, as determined by the value of the tension set, still existed under an applied deformation of up to 200%. Under an applied deformation of 300%, the incorporation of TLCP could not exceed 20 wt % if the elastic property was to be maintained.
5. The results from a dynamic mechanical analysis of the blends revealed a significant improvement in  $E'$ . In particular, in the blend containing 30 wt % TLCP, the moduli in the rubbery states increased by a factor of 7 over that of neat SEBS.

This was attributed to the reinforcement by TLCP fibrils with high aspect ratios.

The authors are indebted to the Alexander von Humboldt Foundation for the donation of the plate-and-plate rheometer and to the Institute of Rubber Research for its permission to use the capillary rheometer.

## References

1. Pawlikowski, G. T.; Dutta, D.; Weiss, R. A. *Ann Rev Mater Sci* 1991, 21, 159.
2. *Rheology and Processing of Liquid Crystalline Polymers*; Arcierno, D.; Collyer, A. A., Eds.; Chapman & Hall: London, 1996.
3. Dutta, D.; Fruitwala, H.; Kohli, A.; Weiss, R. A. *Polym Eng Sci* 1990, 30, 1005.
4. Kiss, G. *Polym Eng Sci* 1987, 27, 410.
5. Nando, G. B.; Gupta, B. R. In *Short Fibre-Polymer Composites*; De, S. K.; White, J. R., Eds.; Woodhead: Cambridge, 1996; p 84.
6. Amornsakchai, T.; Sinpatanapan, B.; Bualek-Limcharoen, S.; Meesiri, W. *Polymer* 1999, 40, 2993.
7. Chantaratcharoen, A.; Sirisinha, C.; Amornsakchai, T.; Bualek-Limcharoen, S.; Meesiri, W. *J Appl Polym Sci* 1999, 74, 2414.
8. Saikrasun, S.; Amornsakchai, T.; Sirisinha, C.; Meesiri, W.; Bualek-Limcharoen, S. *Polymer* 1999, 40, 6437.
9. Lorenzo, L.; Ahuja, S. K.; Chang, H. *Polym Prepr (Am Chem Soc Div Polym Chem)* 1988, 29, 488.
10. Verhoogt, H.; Langelaan, H. C.; Van Dam, J.; De Boer, A. P. *Polym Eng Sci* 1993, 33, 754.
11. Verhoogt, H.; Willems, C. R. J.; Van Dam, J.; De Boer, A. P. *Polym Eng Sci* 1994, 34, 453.
12. Machiels, A. G. C.; Denys, K. F. J.; Van Dam, J.; De Boer, A. P. *Polym Eng Sci* 1996, 36, 2451.
13. Cogswell, F. N. *Polymer Melt Rheology: A Guide for Industrial Practice*; Wiley: New York, 1981; p 27.
14. Dealy, J. M.; Wissbrun, K. F. *Melt Rheology and Its Role in Plastics Processing*; VNR: New York, 1990; p 303.
15. Cox, W. P.; Merz, E. H. *J Polym Sci* 1958, 28, 619.
16. Kalika, D. S.; Denn, M. M. *J Rheol* 1987, 31, 815.
17. Utracki, L. A.; Gendron, R. *J Rheol* 1984, 28, 601.
18. Nakinpong, T.; Bualek-Limcharoen, S.; Bhutton, A.; Aungsupravate, O.; Amornsakchai, T. *J Appl Polym Sci* 2002, 84, 561.
19. Taylor, G. I. *Proc R Soc London Ser A* 1934, 146, 501.
20. Bualek-Limcharoen, S.; Sangsuwan, S.; Amornsakchai, T.; Wannoo, B. *Macromol Symp* 2001, 170, 189.
21. *Thermoplastic Elastomers*; Legge, N. R.; Holden, D.; Schroeder, H. E., Eds.; Hanser: Munich, 1987.
22. Halpin, J. C.; Kardos, J. L. *Polym Eng Sci* 1976, 16, 344.
23. Nakamae, H.; Nishino, T.; Kuroki, T. *Polymer* 1995, 36, 2681.
24. Itoyama, K. *J Polym Sci Part B: Polym Phys* 1988, 26, 1845.
25. Sierra, C. A.; Fatou, J. G.; Parellada, M. D.; Barrio, J. A. *Polymer* 1997, 38, 4325.